A Novel Formulation of a Finite Element-Based Particle-in-Cell Method

Z. Crawford, S. O'Connor, J. Luginsland, and B. Shanker

DoE CSGF Program Review

July 16, 2019

Department of Electrical and Computer Engineering
Department of Computational Mathematics, Science, and Engineering
Michigan State University

Outline

Outline

Motivation

PIC Review

Mixed FEM PIC

- EB-PIC
- DH-PIC

Results

Summary

Motivation

Motivation

- Particle in cell methods play an important role in simulating plasma.
- Application in high powered electronics, accelerators, Z-machines, etc.
- Various codes have been around since the 1970's
- Mostly Finite Difference Time Domain (FDTD) based

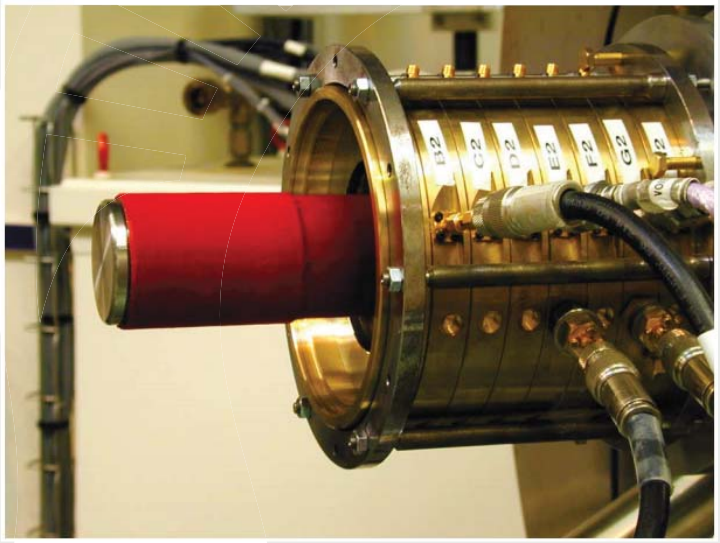

Figure 1: Magnetically insulated line oscillator cathode.[2]

Figure 2: Cavity magnetron by Mr. John Cummings CC-BY-SA 2.0

[2] Cousin et al., "Gigawatt emission from a 2.4-GHz compact magnetically insulated line oscillator (MILO)".

PIC Review

Particle in Cell: Overview

Simulate the behaviour of charge density $\rho(r,t)$ and current density $\mathbf{J}(r,t)$

$$\rho_\alpha(t,\mathbf{r}) = q_\alpha \int f_\alpha(t,\mathbf{r},\mathbf{v})dv$$

$$\mathbf{J}_\alpha(t,\mathbf{r}) = q_\alpha \int \mathbf{v} f_\alpha(t,\mathbf{r},\mathbf{v})dv$$

The distribution function $f_\alpha(t,\mathbf{r},\mathbf{v})$ obeys the Vaslov equation

$$\frac{\partial f_\alpha}{\partial t} + \mathbf{v}\cdot\nabla f_\alpha + \mathbf{a}\cdot\nabla_v f_\alpha = 0 \tag{1}$$

To create Maxwell-Vaslov equation

$$\mathbf{a} = \frac{q_\alpha}{m_\alpha}\left[\mathbf{E} + \mathbf{v}\times\mathbf{B}\right]$$

PIC Cont.

Fields must obey Maxwell's equations

$$\nabla \times \mathbf{E}(\mathbf{r}, t) = -\frac{\partial \mathbf{B}(\mathbf{r}, t)}{\partial t} \tag{2a}$$

$$\nabla \times \frac{\mathbf{B}(\mathbf{r}, t)}{\mu} = \frac{\partial \epsilon \mathbf{E}(\mathbf{r}, t)}{\partial t} + \mathbf{J}(\mathbf{r}, t) \tag{2b}$$

$$\nabla \cdot \mathbf{B}(\mathbf{r}, t) = 0 \tag{2c}$$

$$\nabla \cdot \epsilon \mathbf{E}(\mathbf{r}, t) = \rho(\mathbf{r}, t) \tag{2d}$$

with boundary conditions

$$\hat{n} \times \mathbf{E}(\mathbf{r}, t) = \Psi_E(\mathbf{r}, t) \tag{3a}$$

$$\hat{n} \cdot \mathbf{B}(\mathbf{r}, t) = \Psi_B(\mathbf{r}, t) \tag{3b}$$

PIC Cont.

Self consistent solution, implies (a) map sources, (b) solve MEs, (c) updating particle position, (d) repeat

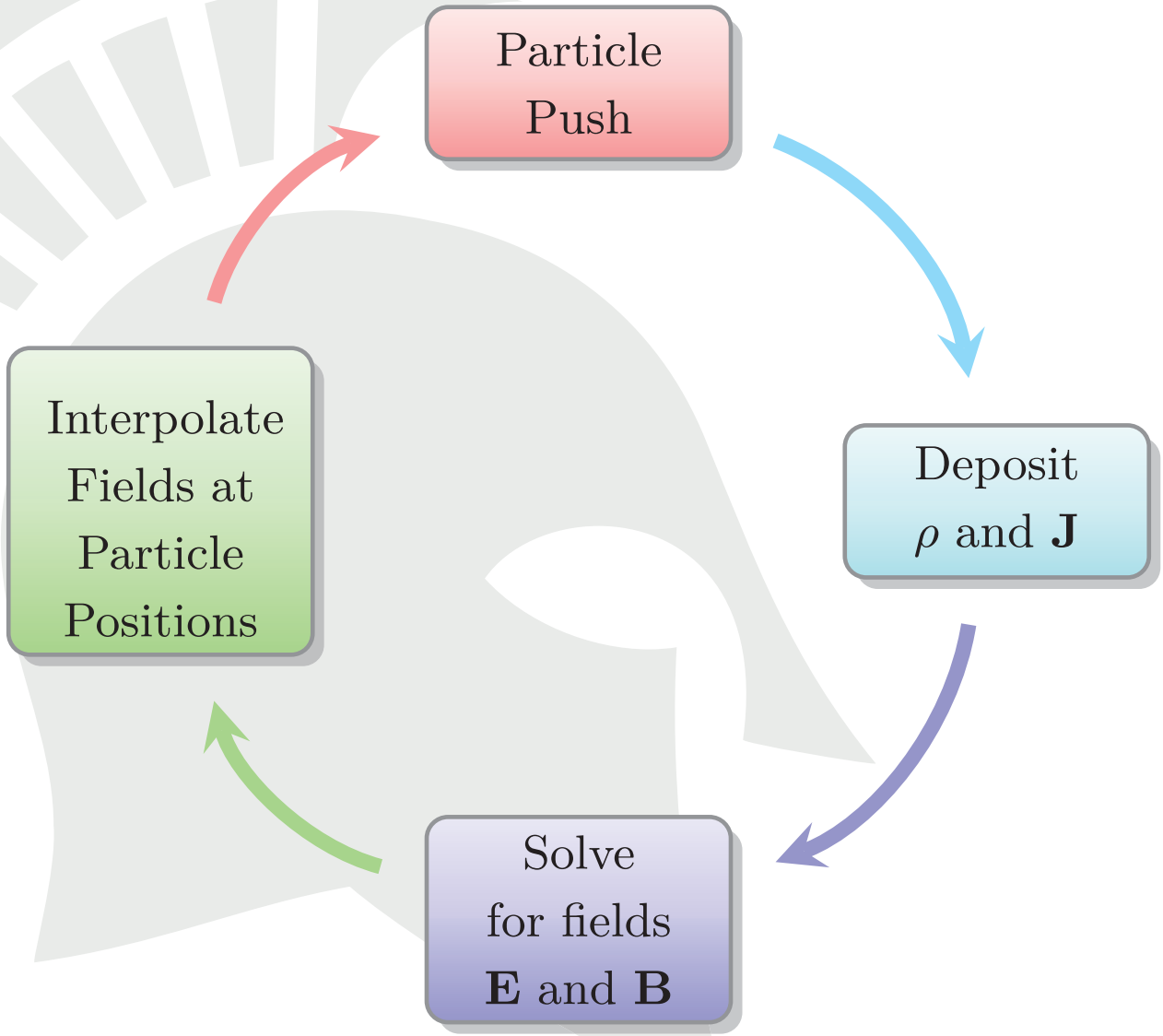

Classical PIC - FDTD

- Relies on Yee cell
  - places **E** and **H** on staggered grid edges
  - places **B** and **D** on staggered grid faces
  - Charge continuity is satisfied
  - No spurious charges are deposited at surfaces

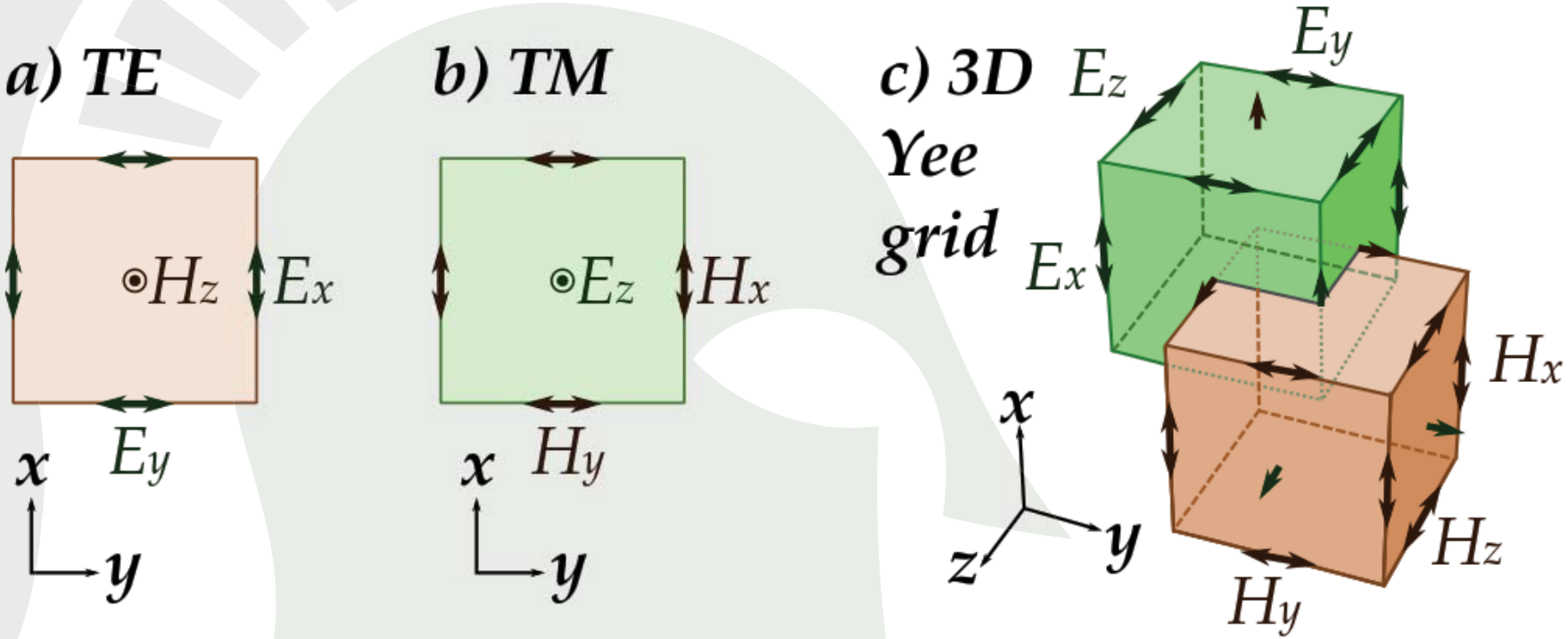

Figure 3: Staggered Yee grids (a-b 2D. c 3D. From https://en.wikipedia.org/wiki/Finite-difference_time-domain_method

Classical PIC - Challenges

- Irregular boundaries are challenging
  - popular-cut cell techniques
- Small time step sizes
- Higher order time and space discretization
- Tempting to invoke FEM

EM FEM

Discretize the vector wave equation

$$\boldsymbol{\nabla} \times \boldsymbol{\nabla} \times \mathbf{E} + \frac{1}{c^2} \frac{\partial^2 \mathbf{E}}{\partial t^2} = -\mu \frac{\partial \mathbf{J}}{\partial t}$$

- TD FEM is challenging
  - Nullspace that grows as $t\nabla\phi$
  - Charge deposition at boundaries
  - Correct mapping were not derived to satisfy charge continuity discretely
  - Several years of unsuccessful efforts

Preliminaries

- Discretize Maxwell's equations instead
- Use different basis functions to represent field and flux quantities $\rightarrow$ mixed representation
- Method developed by
  - Bossavit, Kettunen
  - Monk
  - White
- Application to PIC was pioneered by Sonnendrucker and Tiexeira in 2D

Mixed FEM PIC

Discretized E-B FEM

- The electric field **E** and magnetic flux density **B** are discretized with curl-conforming ($\mathbf{W}^{(1)}$) and divergence-conforming ($\mathbf{W}^{(2)}$) basis functions respectively

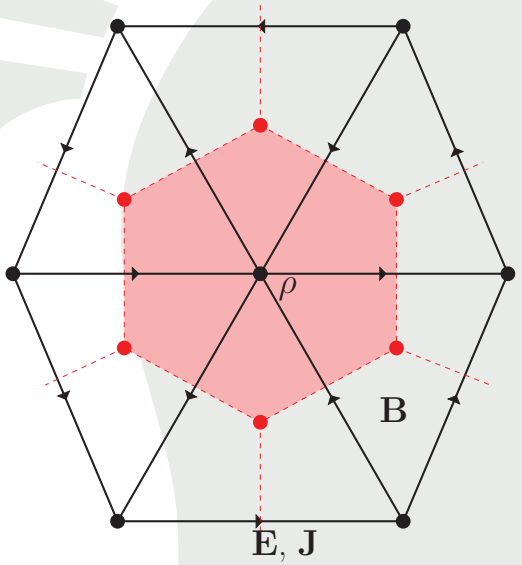

Figure 4: 2D triangular mesh and its dual for **EB** scheme

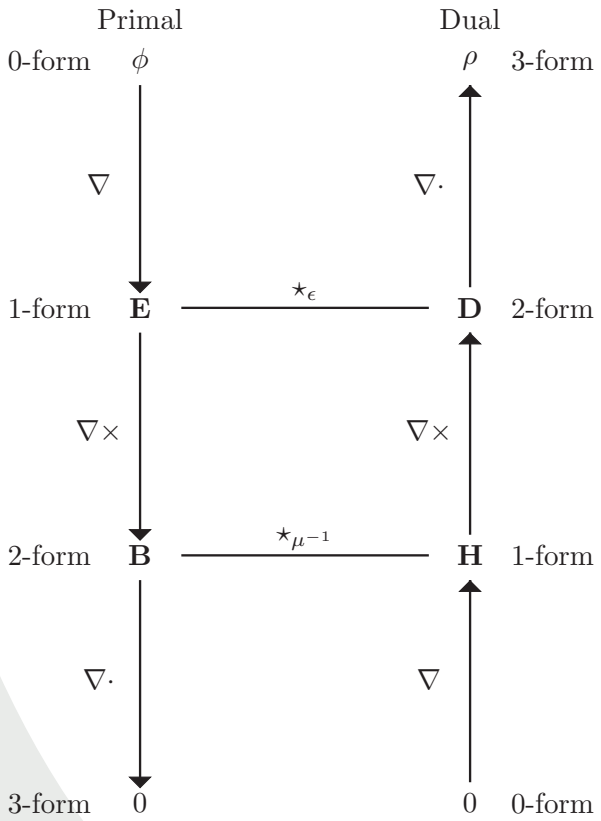

Figure 5: Tonti Diagram of **EB** scheme

Discretized E-B FEM

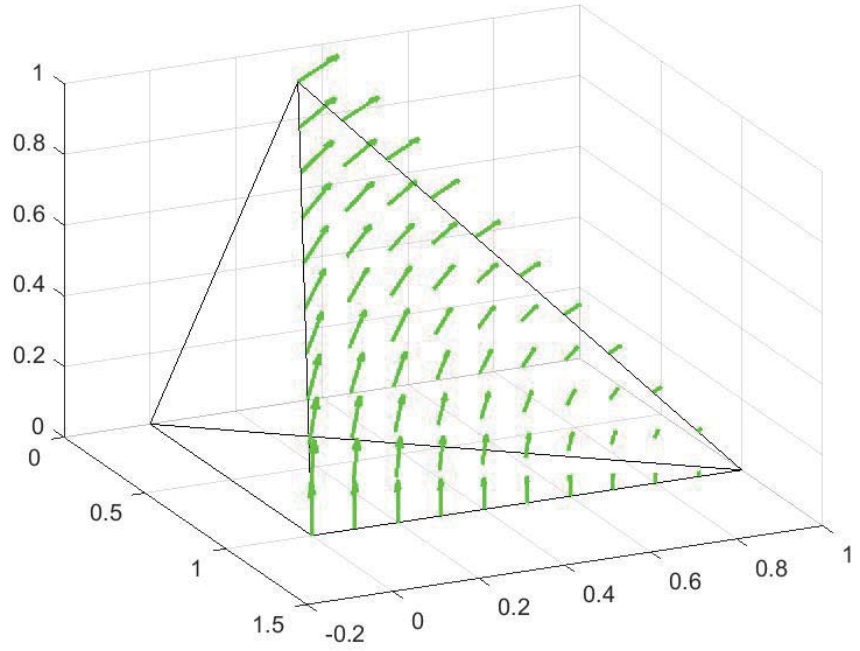

Figure 6: Whitney edge element (for fields). Maintains only *tangential* continuity.

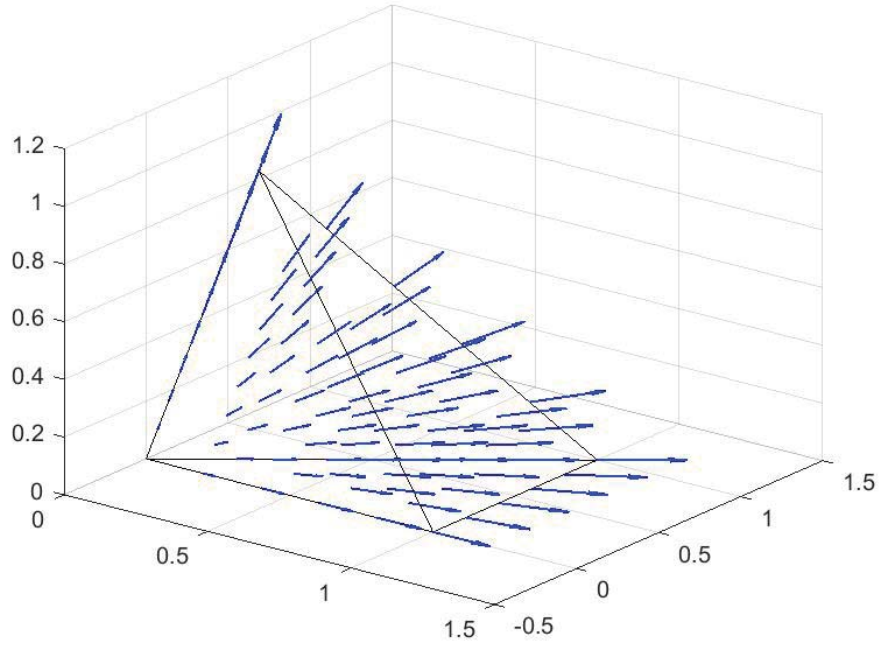

Figure 7: Whitney face element (for fluxes). Maintains only *normal* continuity.

Discretized E-B FEM

$$[D_c]^T[\star_{\mu^{-1}}]\mathcal{B} = \frac{\partial[\star_\varepsilon]\mathcal{E}}{\partial t} + \mathcal{J}_{EB} \tag{4a}$$

$$[D_c]\mathcal{E} = -\frac{\partial \mathcal{B}}{\partial t} \tag{4b}$$

Staggering Faraday's Law and Ampere's law in time to yield the time marching scheme

$$\mathcal{B}^{n+1/2} = \mathcal{B}^{n-1/2} - \Delta_t[D_c]\mathcal{E}^n \tag{5a}$$

$$[\star_\varepsilon]\mathcal{E}^{n+1} = [\star_\varepsilon]\mathcal{E}^n + \Delta_t\left([D_c]^T[\star_{\mu^{-1}}]\mathcal{B}^{n+1/2} - \mathcal{J}_{EB}^{n+1/2}\right) \tag{5b}$$

Current Mapping (neglecting α)

Solution to Vaslov-Maxwell equation has the form

$$f(\mathbf{r}, \mathbf{p}, t) = \sum_s N_s \delta(\mathbf{r} - \mathbf{r}_s(t)) \delta(\mathbf{p} - \mathbf{p}_s(t)) \tag{6}$$

The charge and current densities are defined as

$$\rho(\mathbf{r}, t) = q \int d\mathbf{p} f(\mathbf{r}, \mathbf{p}, t) = q \sum_s N_s \delta(\mathbf{r} - \mathbf{r}_s(t)) \tag{7a}$$

$$\mathbf{J}(\mathbf{r}, t) = q \int d\mathbf{p} \mathbf{v}_s(t) f(\mathbf{r}, \mathbf{p}, t) = q \sum_s N_s \mathbf{v}_s(t) \delta(\mathbf{r} - \mathbf{r}_s(t)) \tag{7b}$$

Current Mapping

Charge conservation requires that

$$\begin{aligned}
\partial_t \rho(\mathbf{r}, t) &= \\
&= q \int d\mathbf{p} \partial_t f(\mathbf{r}, \mathbf{p}, t) \\
&= q \sum_s N_s \partial_t \delta(\mathbf{r} - \mathbf{r}_s(t)) \\
&= -q \boldsymbol{\nabla} \cdot \sum_s N_s \mathbf{v}_s(t) \delta(\mathbf{r} - \mathbf{r}_s(t)) \\
&= -\boldsymbol{\nabla} \cdot \mathbf{J}(\mathbf{r}, t)
\end{aligned} \tag{8}$$

Current Mapping

- Both ρ and $\mathbf{J}$ should be measured by dual space function that are in turn represented in terms of functions in the primal grid.

$$\begin{aligned}\partial_t \langle \lambda_i, \rho \rangle = & \\ &= -\langle \lambda, \boldsymbol{\nabla} \cdot \mathbf{J} \rangle \\ &= \langle \nabla \lambda_i, \mathbf{J} \rangle\end{aligned}$$

In the EB scheme

$$\partial_t \tilde{\rho} = -[D_g]^T \mathcal{J}_{EB}$$

- discrete divergence matrix on the primal grid is equivalent to the transpose of the discrete gradient matrix, $[D_g]$, which has entries of 0 if an edge is not connected to a node, and 1 or -1 if the edge points into or out of a node respectively.

Current Mapping

The measurement of the continuity equation and the particle current must be consistent.

$$\partial_t \tilde{\rho} = \int dV \nabla \lambda \cdot \mathbf{J}$$

Basis definition for Electric Field

$$\mathbf{W}^1_{ij} = \lambda_j \nabla \lambda_i - \lambda_i \nabla \lambda_j$$

Note that

$$\nabla \lambda_i = \mathbf{W}^1_{ij} + \mathbf{W}^1_{ik} + \mathbf{W}^1_{il}$$

and therefore, an operator that sums the particle current measured by the Whitney edge elements would yield a consistent scheme.

Note that the discrete divergence matrix sums the contribution of edges to the nodes where the charge is measured.

This is *independent* of the representation of $\mathbf{J}$.

D-H Finite Element Method

- The choice of discretization for the **EB** scheme represents the electric field and magnetic flux density correctly
- The source quantities are all represented indirectly through a mapping from the dual mesh to the primal mesh.
- Works well under small time step sizes and linear geometry and basis description; Note $\nabla \cdot \mathbf{B} \neq 0$
- Question: Can we reformulate this to avoid these bottlenecks

D-H Finite Element Method

- Solution: **D-H** Mixed FEM
- Current density and charge density now represented on primal grid
- Ampere's Law tested with divergence-conforming basis set; Faraday's law tested with curl-conforming basis set

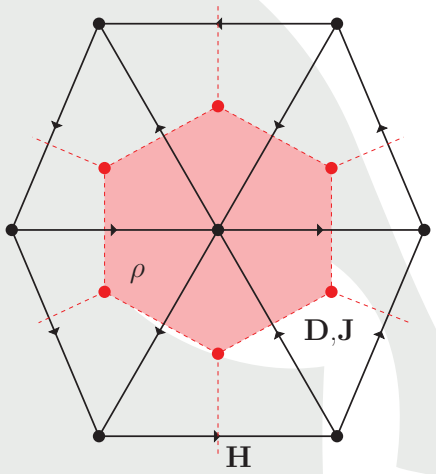

Figure 8: 2D triangular mesh and its dual for **DH** scheme

D-H Finite Element Method

We seek to solve

$$\nabla \times \frac{\mathbf{D}(\mathbf{r},t)}{\epsilon} = -\frac{\partial \mu \mathbf{H}(\mathbf{r},t)}{\partial t} \tag{9a}$$

$$\nabla \times \mathbf{H}(\mathbf{r},t) = \frac{\partial \mathbf{D}(\mathbf{r},t)}{\partial t} + \mathbf{J}(\mathbf{r},t) \tag{9b}$$

$$\nabla \cdot \mu \mathbf{H}(\mathbf{r},t) = 0 \tag{9c}$$

$$\nabla \cdot \mathbf{D}(\mathbf{r},t) = \rho(\mathbf{r},t) \tag{9d}$$

with boundary conditions

$$\hat{n} \times \mathbf{H}(\mathbf{r},t) = \mathbf{J}_s(\mathbf{r},t) \tag{10a}$$

$$\hat{n} \cdot \mathbf{D}(\mathbf{r},t) = \rho_s(\mathbf{r},t) \tag{10b}$$

Discretized D-H FEM

$$[D_c]^T[\star_{\epsilon^{-1}}]\mathcal{D} = -\frac{\partial[\star_\mu]\mathcal{H}}{\partial t} \tag{11a}$$

$$[D_c]\mathcal{H} = \frac{\partial \mathcal{D}}{\partial t} + \mathcal{J}_{DH} \tag{11b}$$

The same staggering in time is used in this formulation, yielding

$$[\star_\mu]\mathcal{H}^{n+1/2} = [\star_\mu]\mathcal{H}^{n-1/2} - \Delta_t[D_c]^T[\star_{\epsilon^{-1}}]\mathcal{D}^n \tag{12a}$$

$$\mathcal{D}^{n+1} = \mathcal{D}^n + \Delta_t\big([D_c]\mathcal{H} - \mathcal{J}_{DH}\big) \tag{12b}$$

Current Mapping

- From current continuity

$$\partial_t \langle \lambda_i, \rho \rangle = \langle \nabla \lambda_i, \mathbf{J} \rangle$$

- In the DH scheme, we write

$$\partial_t \tilde{\rho} = -[D_d] \mathcal{J}_{DH}$$

- Divergence matrix $[D_d]$ has entries of 1 or -1 if a face normal points out of or into a tetrahedron, respectively. Otherwise, the value is zero.
- Trivial to define loop and star structures for $\mathbf{D}$ and co-tree for $\mathbf{H}$ to properly capture the rotational and irrotational components of the velocity.

Current Mapping

- The discrete current mapping in the DH scheme is defined as

$$\begin{aligned}\mathcal{J}_{DH,i} &= q \int dS \hat{n}_i \cdot \mathbf{v}_p(t) \delta(\mathbf{r} - \mathbf{r}_p(t)) \\ &= q \hat{n}_i \cdot \mathbf{v}_p(t)\end{aligned}$$

  if Ampere's Law is discretized by testing with face normals.

- Alternatively, Ampere's law can be tested with the divergence-conforming basis set $\mathbf{W}^{(2)}$ such that

$$\begin{aligned}\mathcal{J}_{DH,i} &= q \int d\Omega \mathbf{W}_i^{(2)}(\mathbf{r}) \cdot \mathbf{v}_p(t) \delta(\mathbf{r} - \mathbf{r}_p(t)) \\ &= q \mathbf{W}_i^{(2)}(\mathbf{r}_p(t)) \cdot \mathbf{v}_p(t)\end{aligned}$$

Current Mapping

The measurement of the continuity equation and the particle current must be consistent. Consider for the lowest order scheme, where surface testing is done for Faraday's law.

$$\int dV \, \partial_t \rho = -\int dV \, \boldsymbol{\nabla} \cdot \mathbf{J}$$

$$\partial_t \tilde{\rho} = -\int dS \hat{n} \cdot \mathbf{J}$$

Again, the measurement scheme of the current is consistent with the measurement of the continuity equation.

Here, the discrete divergence matrix sums contributions from each face for a particular tetrahedron.

Again, this is *independent* of the representation of $\mathbf{J}$.

Results

Basic Particle Motion

- Investigate single particle motion to validate particle pusher.
- Uniform external magnetic flux density $B = 6.82272 \cdot 10^{-5}\hat{z}$ Wb/m^2 is applied with no electric field.
- Macro particle consists of a single electron
- Initial velocity $\mathbf{v} = 3 \cdot 10^6 \hat{\mathbf{y}}$ and position $\mathbf{r} = [0, 0.25, 0]$ which results in a gyro-radius of 0.5 m.

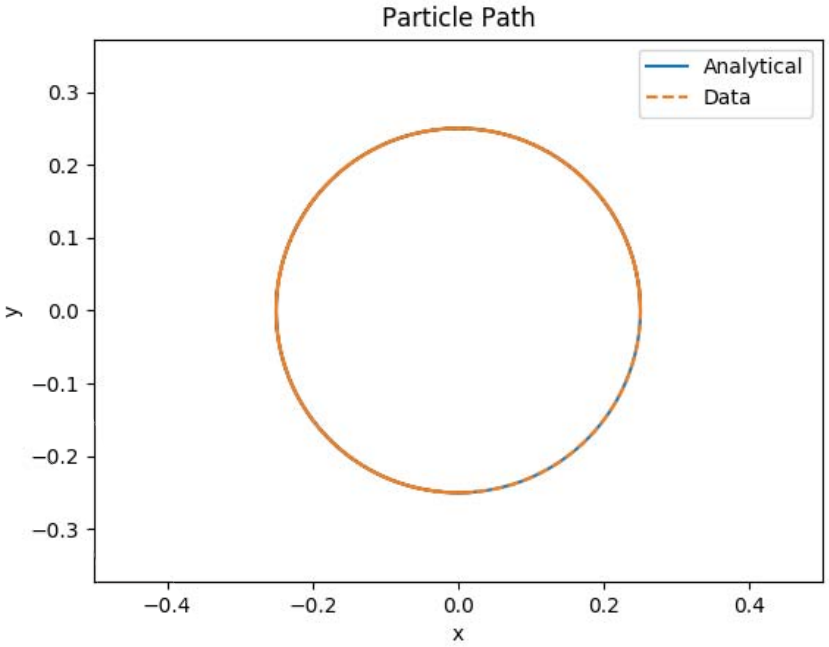

Basic Particle Motion

- Error in particle motion with $dt = 46.1ps$ is around 10^{-4}
- Error for a single particle are dominated by boris push

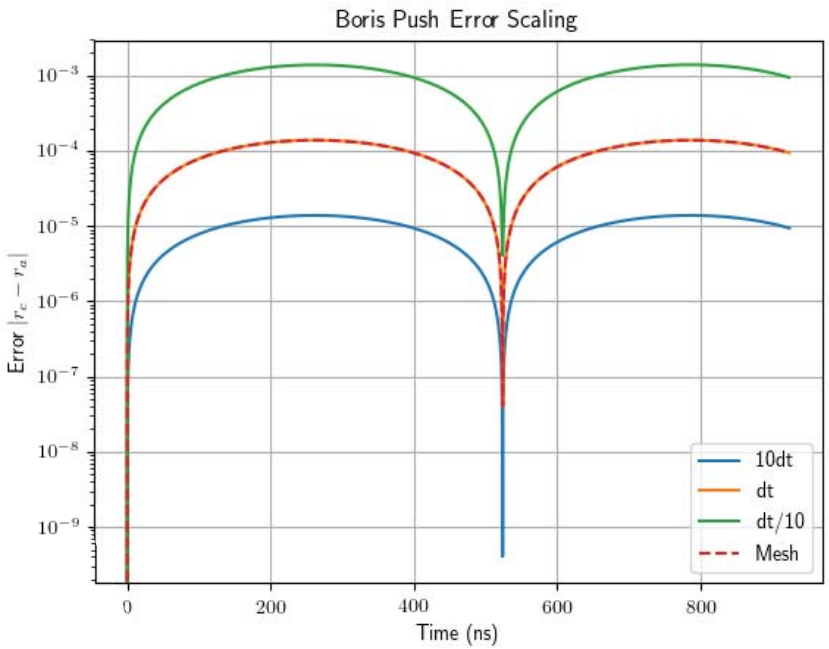

Figure 9: Basis Particle Motion - Error in position over time $|r_c - r_a|$

Basic Particle Motion - DH

Same experiment setup using the **DH** scheme with similar results with two different methods of defining the current mapping

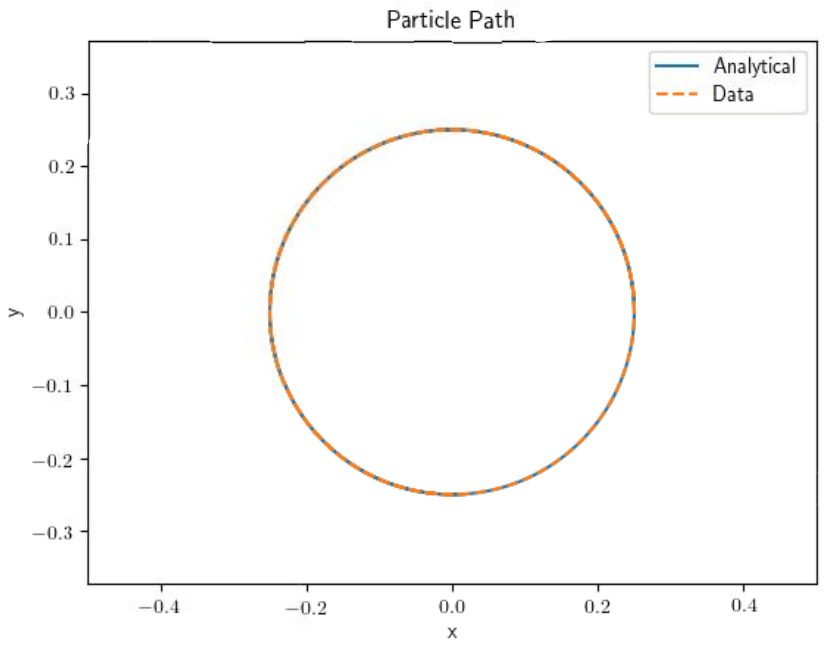

Figure 10: Basic Particle Motion - for DH scheme with current tested by surface normals

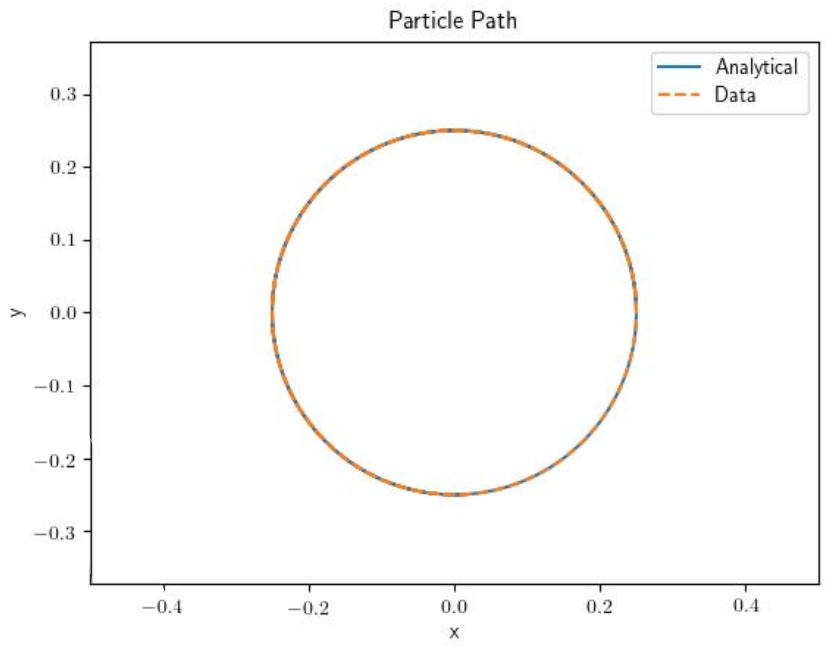

Figure 11: Basic Particle Motion - for DH scheme with current tested by $\mathbf{W}^{(2)}$

Basic Particle Motion - DH

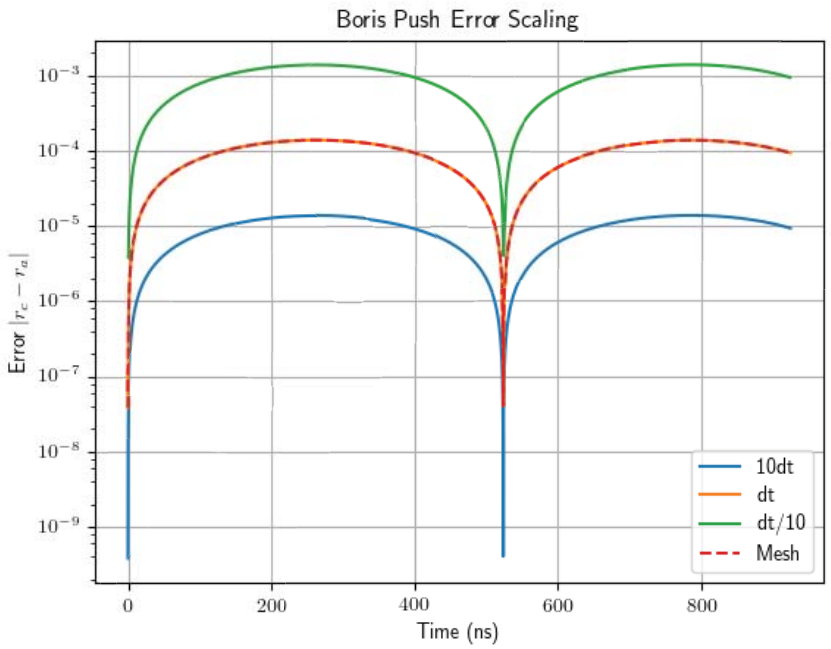

Figure 12: Basic Particle Motion - Error in position over time $|r_c - r_a|$ for DH scheme with current tested by surface normals

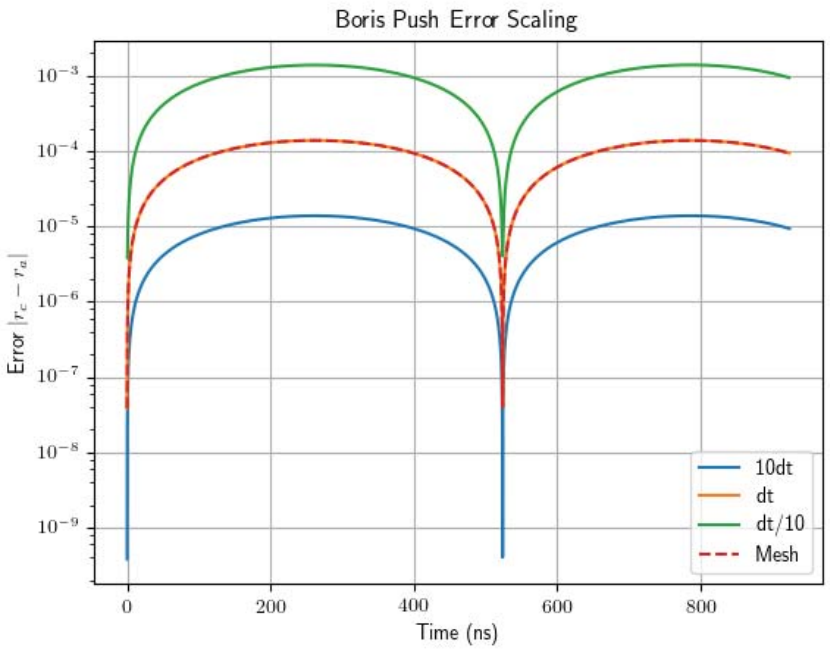

Figure 13: Basic Particle Motion - Error in position over time $|r_c - r_a|$ for DH scheme with current tested by $\mathbf{W}^{(2)}$

Single particle motion with the **DH** scheme for 200,000 time steps

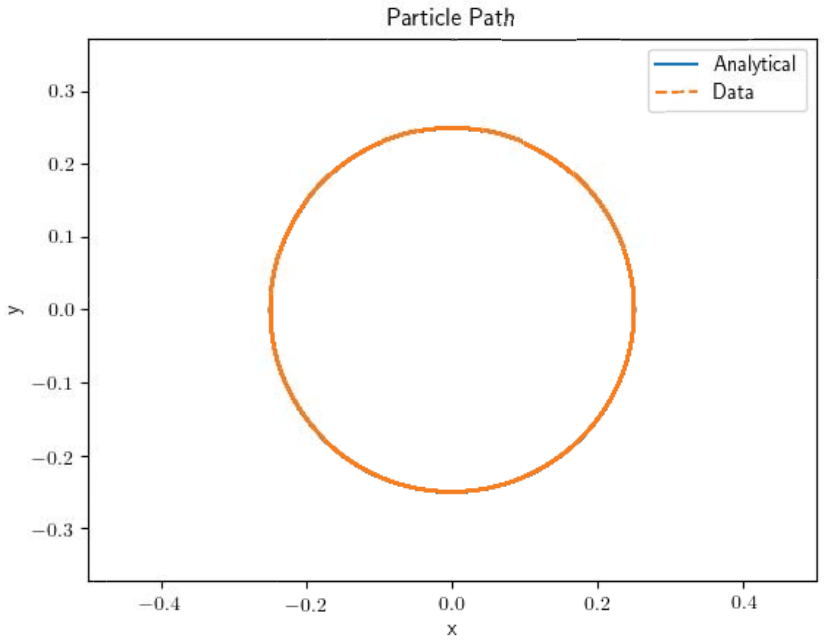

Figure 14: Basic Particle Motion - for DH scheme with current tested by surface normals

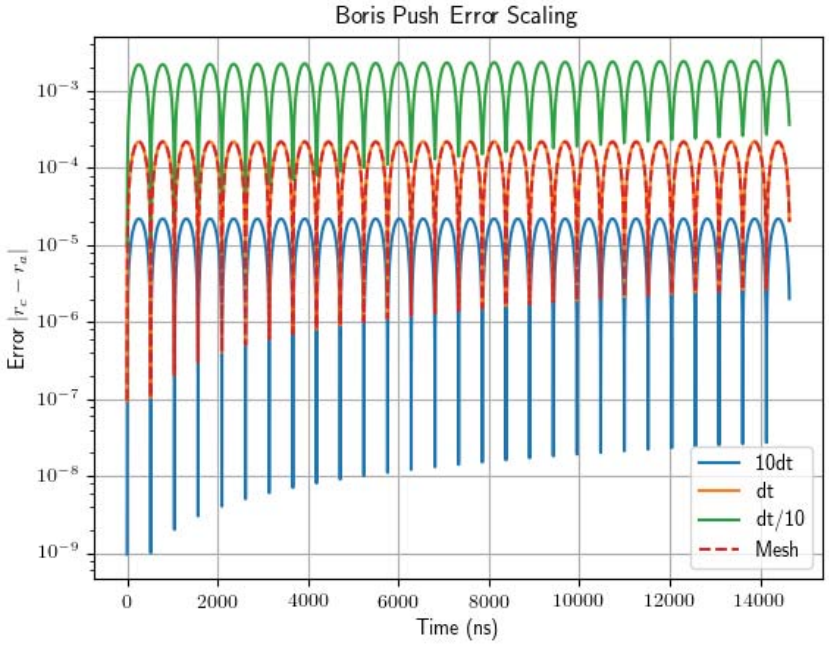

Figure 15: Basic Particle Motion - Error in position over time $|r_c - r_a|$ for DH scheme with current tested by surface normals

Plasma Ball

Adiabatic plasma expansion in a vacuum with initial thermal velocity maxwellian.

- Radius 0.05 m
- Centered in 1x1x1 m PEC box
- ions and electrons overlap at t=0

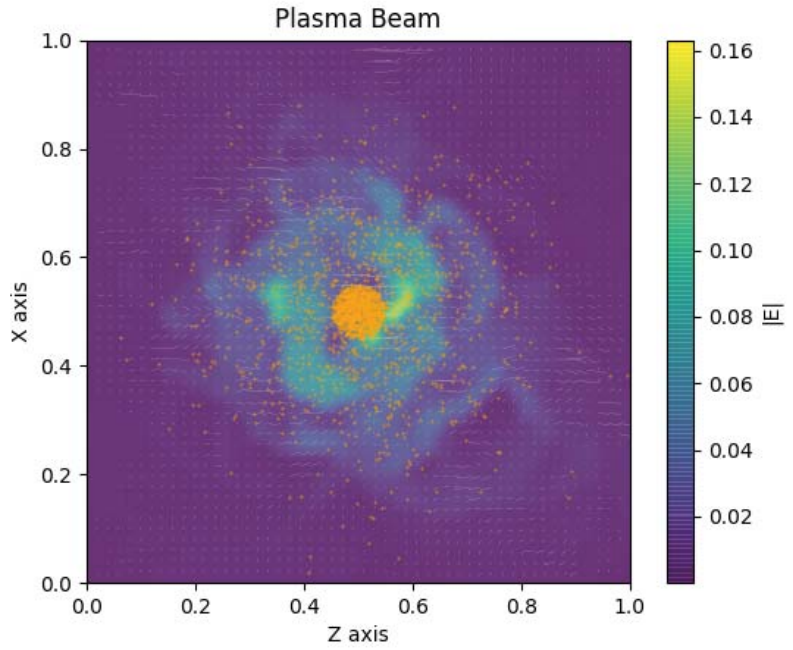

Figure 16: Plasma ball test case - ions located at the center with electrons moving outward at $t = 64.6$ ns

Particle Beam

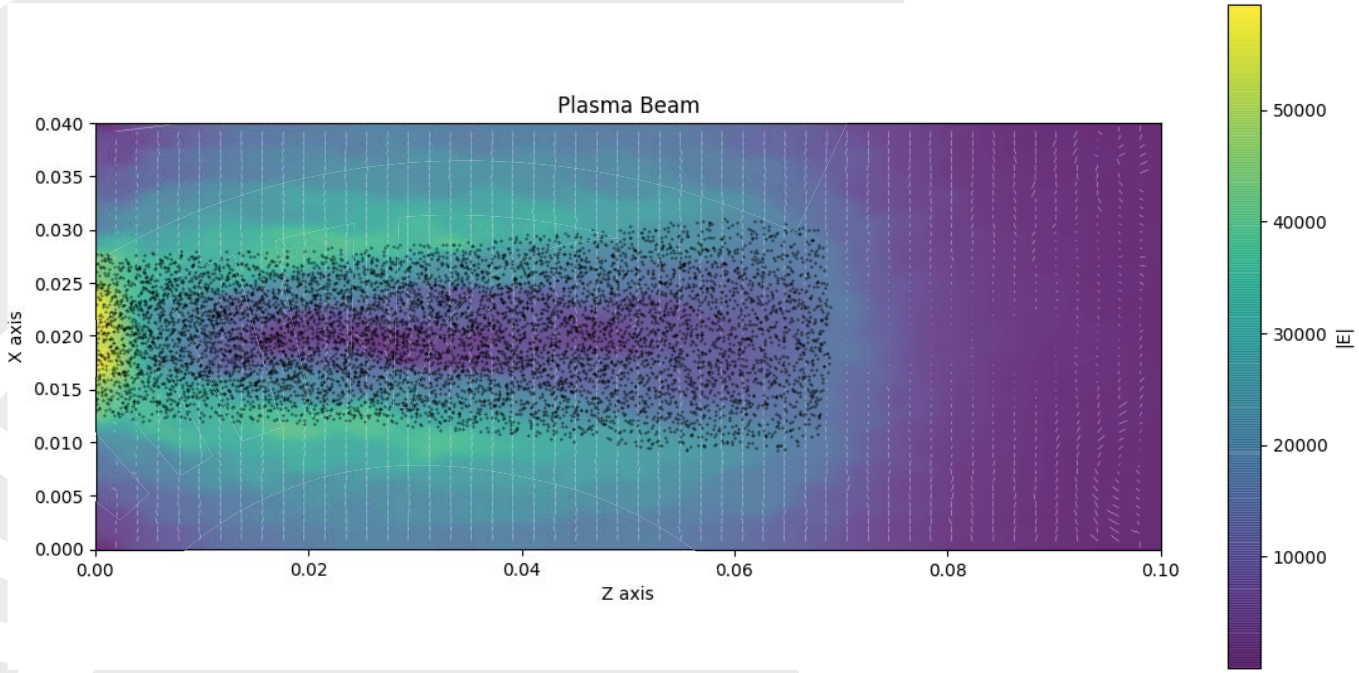

Figure 17: Particle beam test case with electric field magnitude plotted.

Particle beam entering cylindrical tube with PEC boundary conditions

- Beam Current 1A
- Beam Voltage 7.107kV ($\approx 49 \cdot 10^6$ m/s)
- Beam Radius 8 mm
- Macro-particle size 1,040,251
- Time Step 0.5 (ns)
- Mesh Size 0.1 meters
- PEC cylinder geometry radius of 0.04 m and length 0.1 m

Plasma Beam-Validation (?)

- Validation of FEMPIC and XOOPIC (2D code) beam case.
- Particle current continuity equation satisfied.

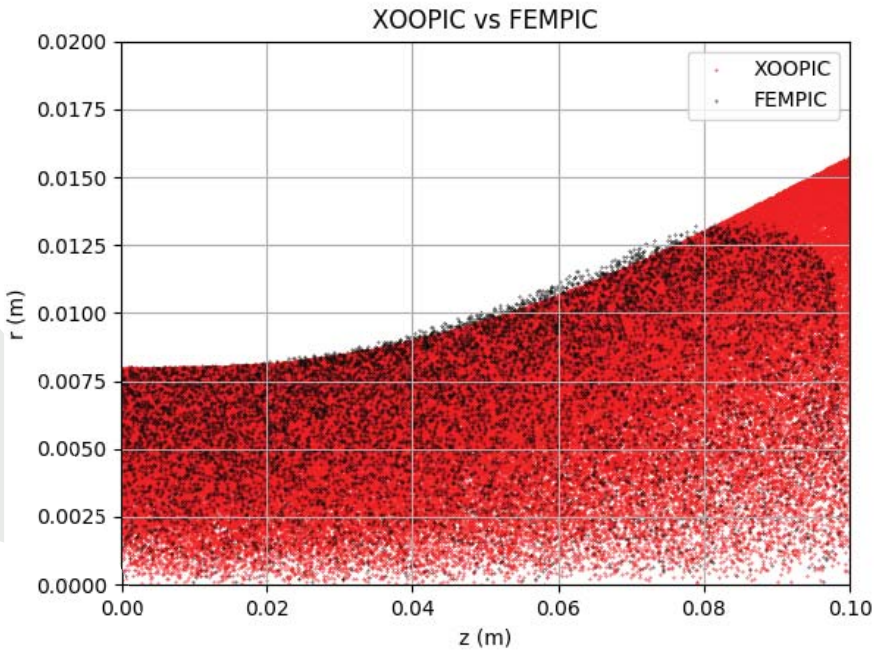

Figure 18: Particles in r-z compared with XOOPIC (red)

Plasma Beam - Current Continuity

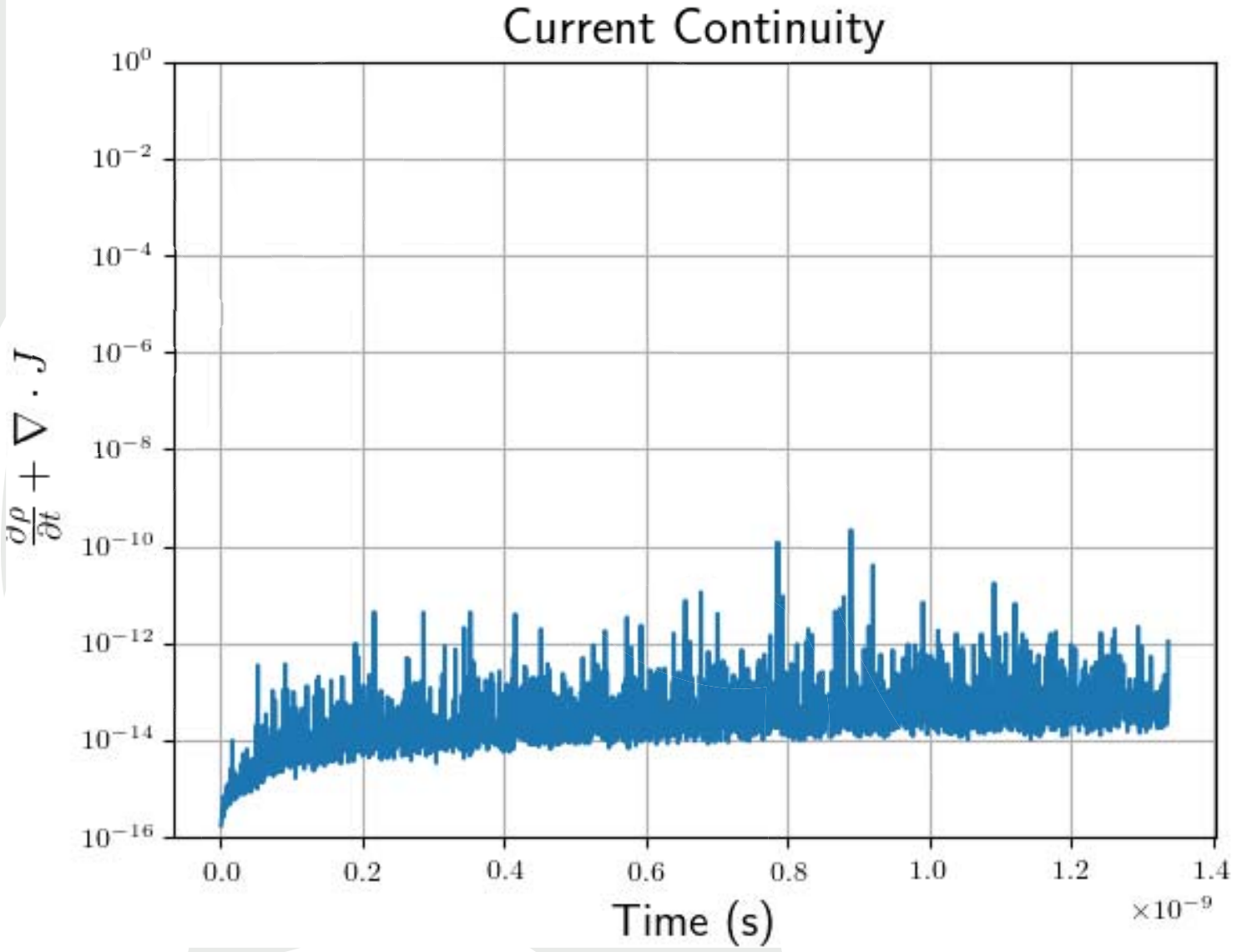

Figure 19: Continuity equation at each time step

Summary

Summary

- Rigorous definition of current mapping for Whitney spaces
- Formulation of a new method
- Developing a sequence of 3D benchmark tests
- All test run so far show proper satisfaction of Gauss' law (and therefore, current continuity)
- No divergence cleaning
- Things to do
  - Develop a sequence of more benchmark tests
  - Extend to periodic system
  - Develop quasi-Helmholtz decompositions

Acknowledgement

This work was supported by the DoE CSGF under grant number DE-FG02-97ER25308.

emrg
Electromagnetics Research Group
Michigan State University

CMSE